Numerical Solution of Plateau's Problem by a Finite Element Method

By Masahiro Hinata, Masaaki Shimasaki and Takeshi Kiyono

Abstract. This paper concerns the application of a finite element method to the numerical solution of a nonrestricted form of the Plateau problem, as well as to a free boundary problem of Plateau type. The solutions obtained here are examined for several examples and are considered to be sufficiently accurate.

It is also observed that the hysteresis effect, which is a feature of a nonlinear problem, appears in this problem.

1. Introduction. Methods for the numerical solution of the Plateau problem have so far been examined by D. Greenspan [3], [4], using the combination technique of difference and variational methods, and by P. Concus [5], using a finite difference method.

These two methods can be applied only to the so-called restricted form of the Plateau problem described by Forsythe and Wasow [2, Section 18.9], that is, to the problems where the boundary condition is represented by a single-valued function. Thus, they cannot be applied to the problem where the boundary condition is represented by a multi-valued function, such as Courant's example described later.

This paper shows that such multi-valued boundary-value problems can be solved numerically by a finite element method. In this case, two solution methods, one for a free boundary problem and the other in a cyclindrical coordinate system, are presented.

2. Application of a Finite Element Method to the Plateau Problem. The Plateau problem involves finding a twice continuously differentiable function $u(x, y)$ in a region D satisfying

(2.1)
$$\left. \begin{aligned} u(x, y) &= f(x, y), \quad \text{or} \\ \partial u(x, y)/\partial x &= g(x, y) \\ \partial u(x, y)/\partial y &= h(x, y) \end{aligned} \right\} \quad \text{on } \partial D$$

and minimizing the surface area functional

(2.2)
$$Ju = \iint_D (1 + u_x^2 + u_y^2)^{1/2} \, dx \, dy,$$

where $f(x, y)$, $g(x, y)$ and $h(x, y)$ are single-valued functions [2, Section 18.9].
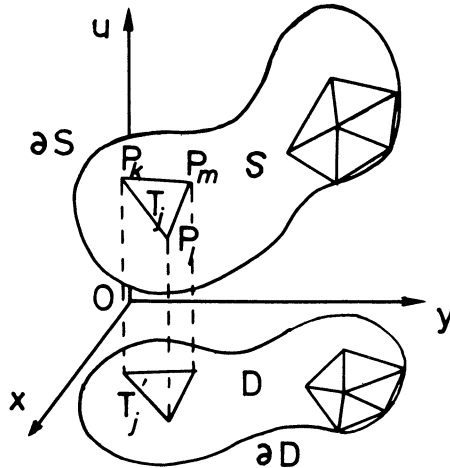
FIGURE 1. *A coordinate system*

A finite element method is applied to the Plateau problem in the following manner: Consider a linear basis function $u_i(x, y)$ written in the form

$$(2.3) \qquad u_i(x, y) = A_i x + B_i y + C_i.$$

The coefficients A_i, B_i and C_i in Eq. (2.3) can be determined by three points in the x-y-u space. Let D be approximated by the union of disjoint triangles T_j' ($j = 1, \cdots, Q$). Let the three vertices of T_j' in the x-y plane be $P_k'(x_k, y_k, 0)$, $P_l'(x_l, y_l, 0)$, and $P_m'(x_m, y_m, 0)$ and let the three vertices of a triangle T_j in the x-y-u space corresponding to T_j' be $P_k(x_k, y_k, u_k)$, $P_l(x_l, y_l, u_l)$ and $P_m(x_m, y_m, u_m)$, respectively. Then T_j is represented in the form

$$(2.4) \quad u_i(x, y) = \left(\begin{vmatrix} u_k & y_k & 1 \\ u_l & y_l & 1 \\ u_m & y_m & 1 \end{vmatrix} x + \begin{vmatrix} x_k & u_k & 1 \\ x_l & u_l & 1 \\ x_m & u_m & 1 \end{vmatrix} y + \begin{vmatrix} x_k & y_k & u_k \\ x_l & y_l & u_l \\ x_m & y_m & u_m \end{vmatrix} \right) \bigg/ \begin{vmatrix} x_k & y_k & 1 \\ x_l & y_l & 1 \\ x_m & y_m & 1 \end{vmatrix}.$$

The area of the triangle T_j' is given by

$$(2.5) \qquad \iint_{T_j'} dx\, dy = \tfrac{1}{2} \operatorname{abs} \begin{vmatrix} x_k & y_k & 1 \\ x_l & y_l & 1 \\ x_m & y_m & 1 \end{vmatrix}$$

and the area of the polyhedral surface consisting of the T_j is given by

$$(2.6) \qquad Ju = \tilde{J}u = \sum_{j=1}^{Q} \iint_{T_j'} (1 + u_{jx}^2 + u_{jy}^2)^{1/2}\, dx\, dy$$

$$(2.7) \qquad = \sum_{j=1}^{Q} (1 + A_j^2 + B_j^2)^{1/2} \iint_{T_j'} dx\, dy$$

$$(2.8) \qquad = \sum_{j=1}^{Q} \frac{1}{2} \left[\begin{vmatrix} x_k & y_k & 1 \\ x_l & y_l & 1 \\ x_m & y_m & 1 \end{vmatrix}^2 + \begin{vmatrix} u_k & y_k & 1 \\ u_l & y_l & 1 \\ u_m & y_m & 1 \end{vmatrix}^2 + \begin{vmatrix} x_k & u_k & 1 \\ x_l & u_l & 1 \\ x_m & u_m & 1 \end{vmatrix}^2 \right]^{1/2}.$$
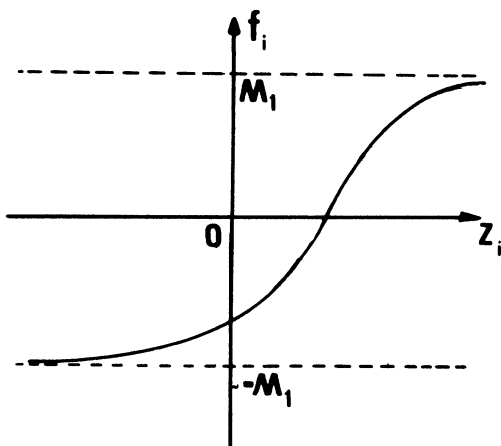
FIGURE 2. *Schematic view of* $f_i(z_1, z_2, \cdots, z_p)$

The problem of finding a twice continuously differentiable function $u(x, y)$, minimizing the continuous functional Ju, can thus be approximated by that of finding a piecewise linear function

$$(2.9) \qquad \bar{u}(x, y) = \sum_{j=1}^{Q} u_j(x, y)\Phi_j(x, y),$$

where

$$(2.10) \qquad \begin{aligned} \Phi_j(x, y) &= 1 \quad \text{in } T_j', \\ \Phi_j(x, y) &= 0 \quad \text{out of } T_j', \end{aligned}$$

minimizing the functional $\tilde{J}u$.

The following fact should be noted. In the finite element method, it is not necessary to fix the T_i', or the division of D; it is only necessary to minimize the functional $\tilde{J}u$, treating the P_i's as unknown points in the (x, y, u)-space. This flexibility is useful in solving various problems, such as free boundary problems. If the variational point $P_i(x_i, y_i, u_i)$ is selected in the direction $(\alpha_i, \beta_i, \gamma_i)$ from the point (x_i^0, y_i^0, u_i^0), that is

$$(2.11) \qquad x_i = \alpha_i z_i + x_i^0, \qquad y_i = \beta_i z_i + y_i^0, \qquad u_i = \gamma_i z_i + u_i^0,$$

where $\alpha_i^2 + \beta_i^2 + \gamma_i^2 = 1$, then the necessary condition for minimizing $\tilde{J}u$ is given by

$$(2.12) \qquad \partial \tilde{J}u/\partial z_i \equiv f_i = 0 \qquad (i = 1, \cdots, p).$$

A numerical analyst can choose the direction of variation in a manner best suited to his problem.

Equations (2.12) are nonlinear algebraic equations, which may be solved iteratively by the generalized Newton method, in which the $(n + 1)$th approximation $z_i^{(n+1)}$ to z_i is determined by

$$(2.13) \qquad z_i^{(n+1)} = z_i^{(n)} - \omega \frac{f_i(z_1^{(n+1)}, \cdots, z_{i-1}^{(n+1)}, z_i^{(n)}, z_{i+1}^{(n)}, \cdots, z_p^{(n)})}{\partial f_i(z_1^{(n+1)}, \cdots, z_{i-1}^{(n+1)}, z_i^{(n)}, z_{i+1}^{(n)}, \cdots, z_p^{(n)})/\partial z_i},$$
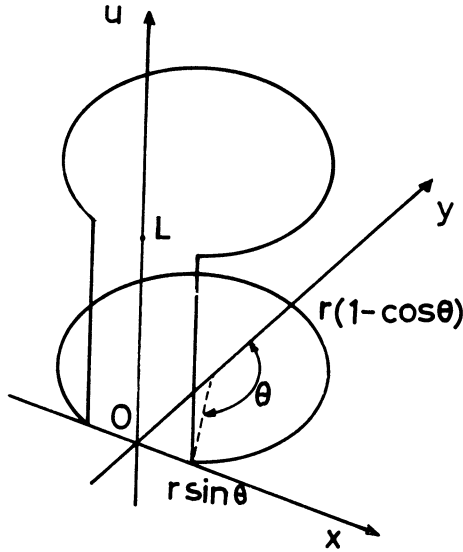
$$(i = 1, \cdots, p);$$

FIGURE 3. *Contour with a multi-valued boundary condition*

here ω is a relaxation parameter which when sufficiently small results in convergence.

We now consider f_i and $\partial f_i/\partial z_i$ in Eq. (2.13). A simple computation gives the following result:

$$(2.14) \qquad\qquad |f_i| < M_1,$$

$$(2.15) \qquad\qquad M_2 > (\partial f_i/\partial z_i) > 0,$$

where M_1 and M_2 are constants.

An outline of f_i as a function of z_i is shown in Fig. 2. This figure shows that when $\partial f_i/\partial z_i$ is extremely small, the generalized Newton method diverges.

3. A Free Boundary Problem. Minimal surface problems with multi-valued boundary conditions cannot be solved numerically by the usual finite difference method [3]–[5]. Certain types of such problems, however, can be reduced to free boundary problems with single-valued boundary conditions. We will now examine such free boundary problems using the finite element method of the previous section. Consider the contour shown in Fig. 3. If $\theta > \pi/2$, the contour cannot be projected in a single-valued fashion and a boundary-value function is not single-valued. To avoid the adverse condition of multi-valuedness, the surface was cut with the plane $x = 0$, taking advantage of the symmetry of the solution (see Fig. 4). Treating only the space $x \geqq 0$, the surface under consideration becomes a single-valued function of u and y, while the cross section of the surface and the u-y plane becomes an unknown boundary curve (the free boundary F in Fig. 4).

As boundary conditions, we have

$$x = r \cdot \sin(\pi - \theta) \quad \text{on } y = 0, \, 0 \leqq u \leqq L,$$

$$(y - r \cdot \cos(\pi - \theta))^2 + x^2 = r^2, \qquad x \geqq 0, \, y \geqq 0 \text{ on } u = 0 \text{ or } L,$$
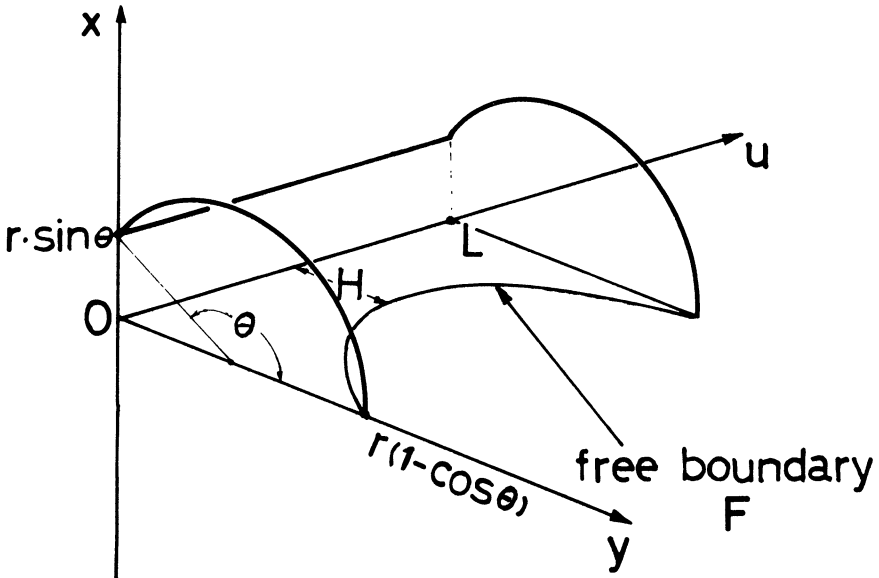
FIGURE 4. *A free boundary scheme*

and, on the free boundary, treating the unknown surface as a function of x and u, we have

$$\partial y/\partial x = 0 \text{ on } x = 0, \quad 0 \leqq u \leqq L.$$

Using the symmetry with respect to $u = L/2$, the boundary conditions are eventually given by

(3.1) $$x = r \cdot \sin \theta \quad \text{on } y = 0 \text{ and } 0 \leqq u \leqq L/2,$$

(3.2) $$x^2 + (y + r \cdot \cos \theta)^2 = r^2 \quad \text{on } u = 0, x \geqq 0, y \geqq 0,$$

(3.3) $$\partial y/\partial u = 0 \quad \text{on } x = 0, 0 \leqq u \leqq L/2,$$

(3.4) $$\partial x/\partial u = 0 \quad \text{on } u = L/2, 0 \leqq y \leqq H,$$

where the unknown height H from the plane $y = 0$, i.e., the x-u plane, is determined by solving the above boundary problem.

On the free boundary F, the unknown variables are $y_{M,j}$ $(j = 1, \cdots, N)$, while in the region D, the unknown variables are x_j $(j = 1, \cdots, p - N)$. Then the y-component of the point on the curve F must be largest in y-components of points in D which have the same u-component, and in the present program, $y_{i,j}$ is given by

(3.5) $$y_{i,j} = y_{M,j} \cdot y_{i,0}/y_{M,0}$$

(see Fig. 5). Thus, the division of the region varies during the generalized Newton iterations and this flexibility is the key to the successful investigation of the free boundary problem.

We now describe some numerical examples. Here

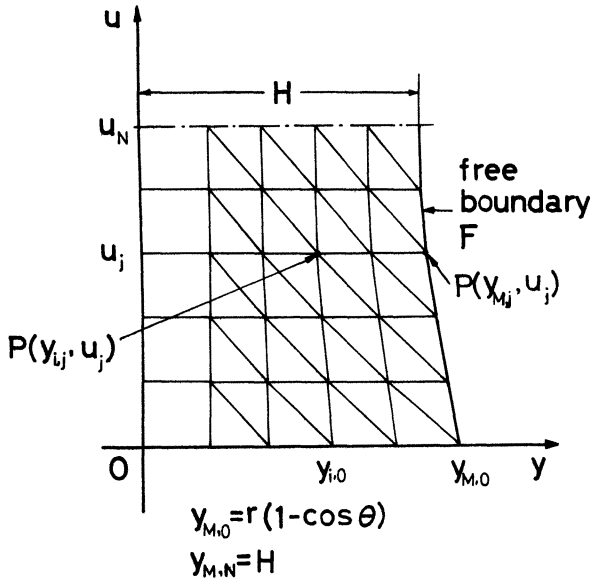$$u_j = j\Delta u, \quad \Delta u = L/(2N), \quad j = 0, 1, \cdots, N,$$

and

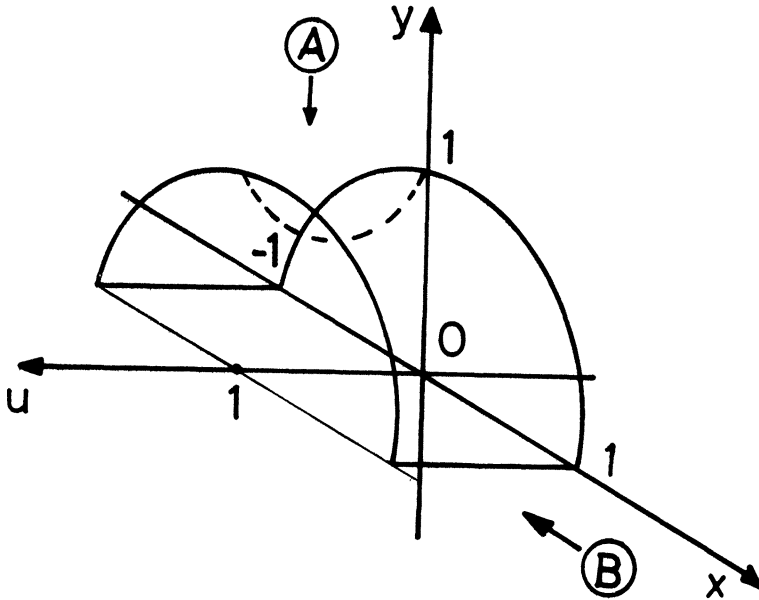FIGURE 5. *Division of the region for the free boundary problem*

FIGURE 6. *Two directions of projection for the case $\theta = \pi/2$*

$$y_{i,0} = r\{1 - \cos(i\Delta\theta)\}, \qquad \Delta\theta = \theta/M, \ i = 0, 1, \cdots, M.$$

Example 1. $\theta = \pi/2$, $r = 1.0$, $L = 1.0$. This boundary-value problem was first solved numerically in direction A (see Fig. 6) using Greenspan's method for which a theoretical analysis is given in [6]. The problem was then solved in direction B with the present free boundary program. For comparison, numerical results given by these two methods are seen in Table 1, where the initial approximations are both

TABLE 1. *Comparison of two methods*

	A	B
H	0.8552107	0.8551592
Area (1/4)	0.7571279	0.7571000
Relaxation parameter	1.2*	1.2*
Iterations to convergence	144	221
Number of arc divisions: $M(\Delta\theta)$	15(6°)	15(6°)
Number of $L/2$ divisions: N	7	7

* In this table, the initial relaxation parameter is 1.2, and δ, the termination parameter for iterations is 10^{-7}. When $\max_{1 \leq i \leq p} |z_i^{(n+1)} - z_i^{(n)}| < \delta$, the iteration process is stopped.

cylindrical, namely

$$(3.6) \qquad x^2 + y^2 = 1, \qquad y \geq 0, 0 \leq u \leq L,$$

Example 2. Catenoid. The second example is that of the catenoid. The soap film with this boundary condition is shown in Fig. 7. This problem can also be solved as a free boundary problem with boundary conditions (3.2)–(3.4) and the Neumann condition

$$(3.1') \qquad \partial x/\partial y = 0 \quad \text{on } y = 0 \text{ and } 0 \leq u \leq L/2$$

in place of (3.1); here $\theta = \pi/2$.
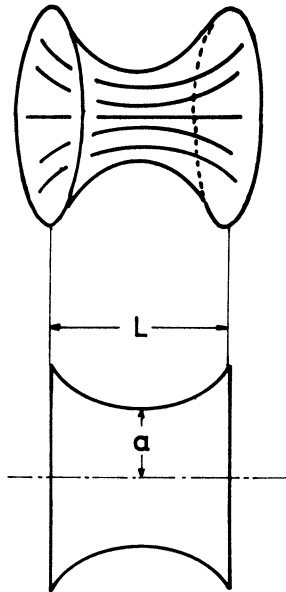
L and a in Fig. 7 are connected by the relation

FIGURE 7. *Catenoid*

TABLE 2. *Comparison of two values of a*

| | | *a* | |
| | | | Value from free |
$L/2$	Value from Eq. (3.7)		boundary program
0.3	0.9523568		0.9520186
0.4	0.9107381		0.9100505
0.5	0.8483438		0.8470727
0.6	0.7450713		0.7423604
0.63	0.6937394		0.6894363
0.66	0.5941309		0.5739461
0.67	no value		no value

(3.7) $$a \cdot \cosh(La/2) = 1$$

and L must necessarily satisfy the relation

(3.8) $$L/2 \leqq \lambda_0/\cosh \lambda_0,$$

where λ_0 is the root of the equation

(3.9) $$\lambda = \coth \lambda.$$

It is seen that λ_0 is nearly equal to 1.2, so that $\lambda_0/\cosh \lambda_0$ is nearly equal to 0.66. For comparison, two computed values of a are given in Table 2. One value was obtained from Eq. (3.7) and the other was computed as H using the present free boundary program ($\Delta u = 0.1$, $\Delta \theta = 10°$). In this case again, the results of the present computer programs are close to the actual values.

Example 3. *An example of R. Courant.* We now apply the finite element method to the interesting contour shown in Figs. 8, 9, and Fig. 3, for $\theta > \pi/2$. The soap film problem may have two different solutions, depending on the length of the line L and the angle of arc θ ($\theta > \pi/2$) (see Figs. 8, 9). Let $\theta = 5\pi/6$, $r = 1.0$ and L vary in Fig. 3. This boundary may sometimes be spanned by two different soap films
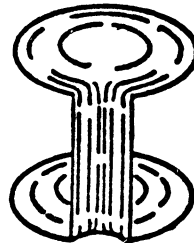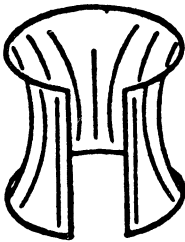

FIGURE 8. *A solution of the soap film problem*   FIGURE 9. *Another solution of the soap film problem*
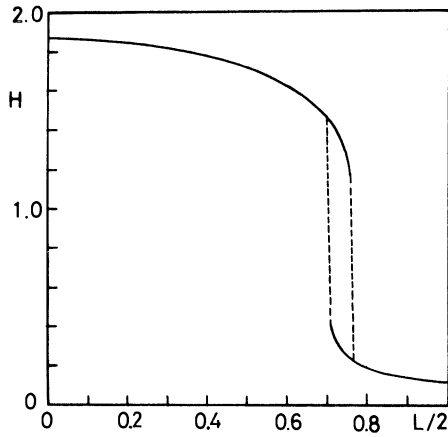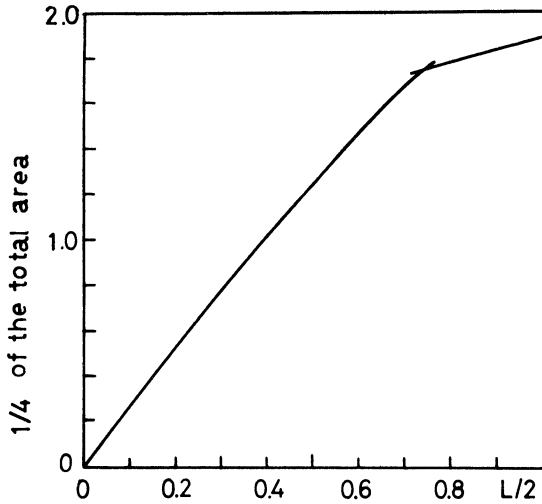
FIGURE 10. *Relation between L and H*

FIGURE 11. *Relation between L and 1/4 of the total area*

which we will now compute with the present free boundary program. The relation between L and H, obtained by numerical computation, is shown in Fig. 10 and the relation between L and $1/4$ of the total area in Fig. 11. Figures 10 and 11 show the hysteresis effect, which is a feature of a nonlinear problem.

We define the nth norm $N^{(n)}$ of solutions, the nth refinement $R^{(n)}$ and the nth eigenvalue $\eta^{(n)}$, by

$$(3.10) \qquad N^{(n)} = \left(\sum_{i=1}^{p} (z_i^{(n)})^2 \right)^{1/2},$$

$$(3.11) \qquad R^{(n)} = \mathrm{abs}(N^{(n)} - N^{(n-1)})$$

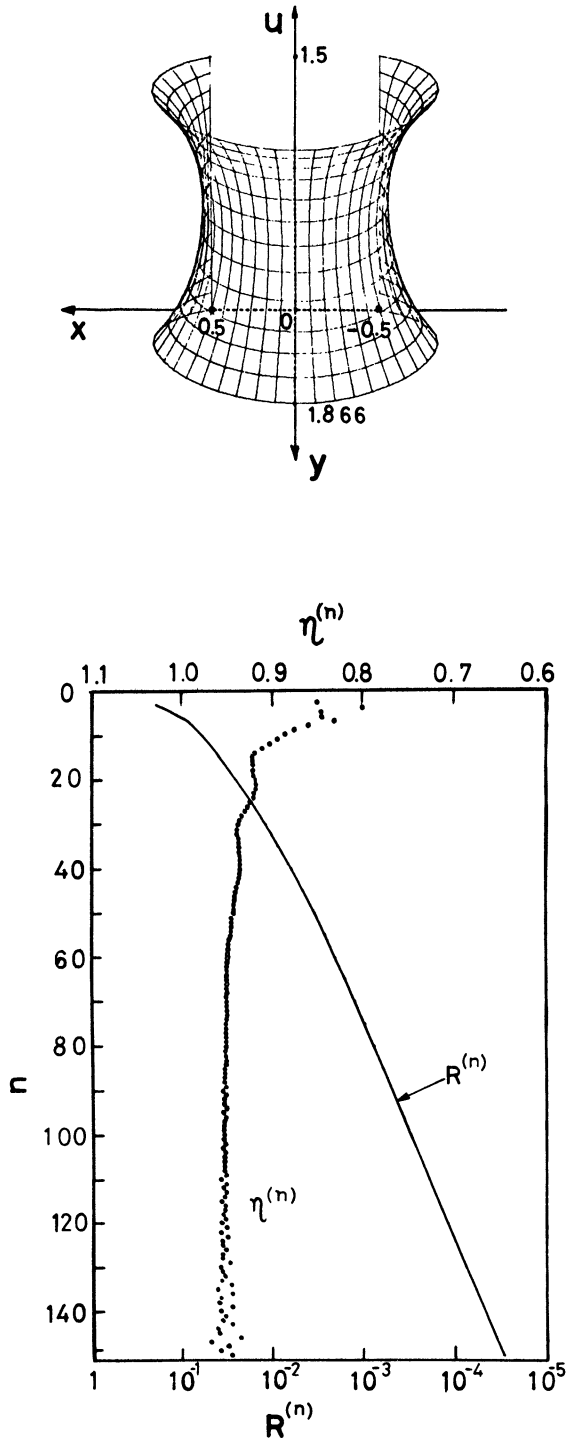and

$$(3.12) \qquad \eta^{(n)} = R^{(n)}/R^{(n-1)},$$

FIGURE 12. *A solution for $L = 1.5$ obtained by starting from an initial approximation of the cylinder* $x^2 + (y + \cos(5\pi/6))^2 = 1$
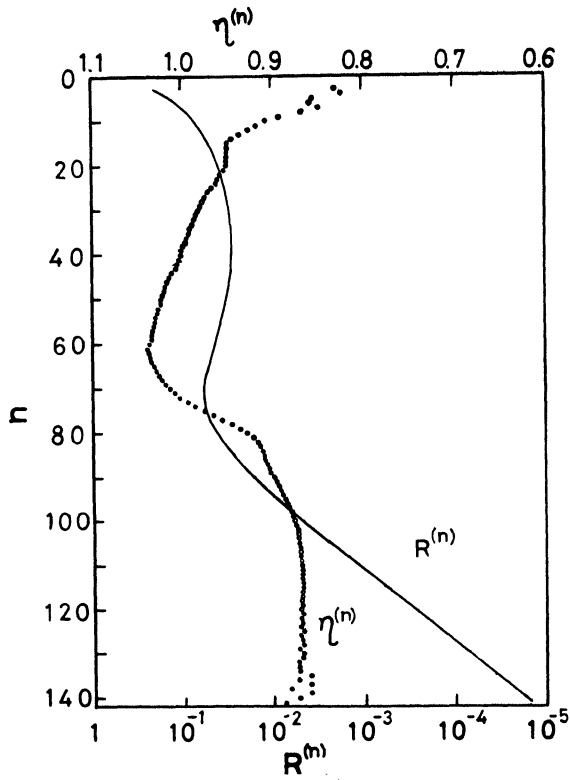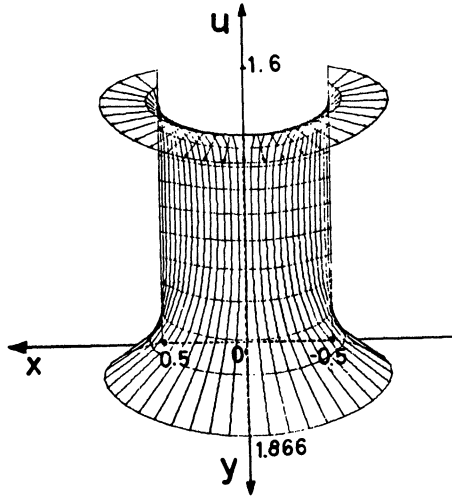
FIGURE 13. *A solution for* $L = 1.6$ *obtained by starting from an initial approximation of the cylinder* $x^2 + (y + \cos(5\pi/6))^2 = 1$

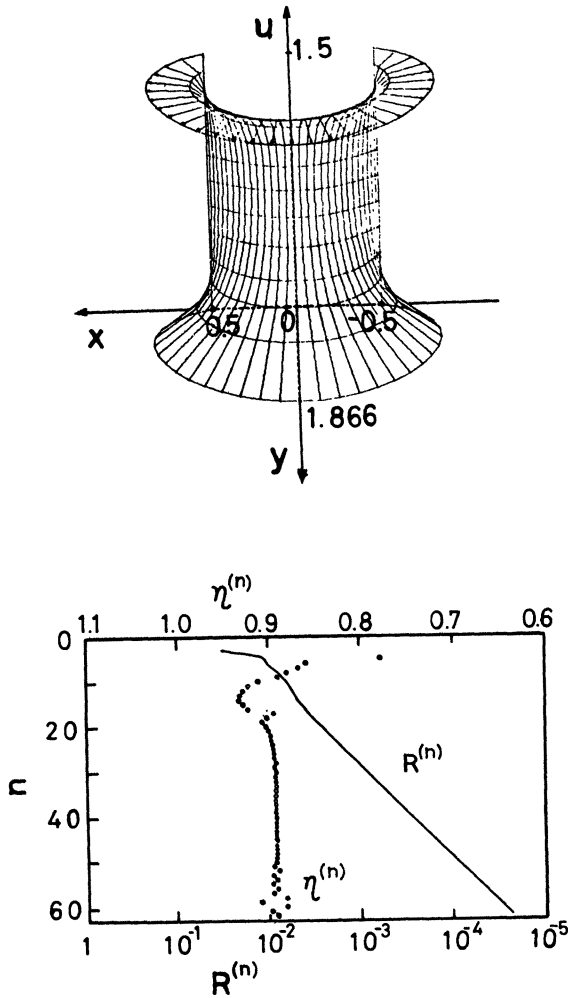FIGURE 14. *Another solution for L = 1.5. This solution can be obtained by using the solution for L = 1.6 shown in Fig. 16 as a starting approximation for this problem*

respectively, where p is the number of all unknown variables z_i. We show the starting approximation, the final approximate solution (converged) and $R^{(n)}$, $\eta^{(n)}$ in each iteration for two different solutions for $L = 1.5$ in Figs. 12 and 14, respectively, where $\delta = 10^{-5}$. The solution for $L = 1.5$, shown in Fig. 14, was obtained starting from the final solution for $L = 1.6$ shown in Fig. 13.

4. Cylindrical Coordinate System. We next consider the foregoing problem in cylindrical coordinates.

To avoid the boundary condition function being two-valued, this boundary is cut with the plane $u = u_i$ ($0 \leqq u_i \leqq L$) (see Fig. 15) and a cross section is shown in Fig. 16.
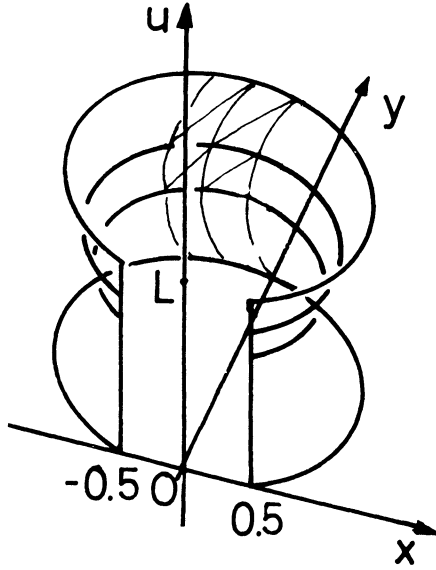
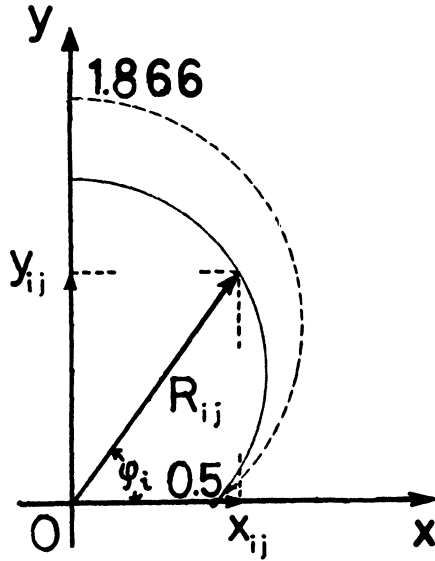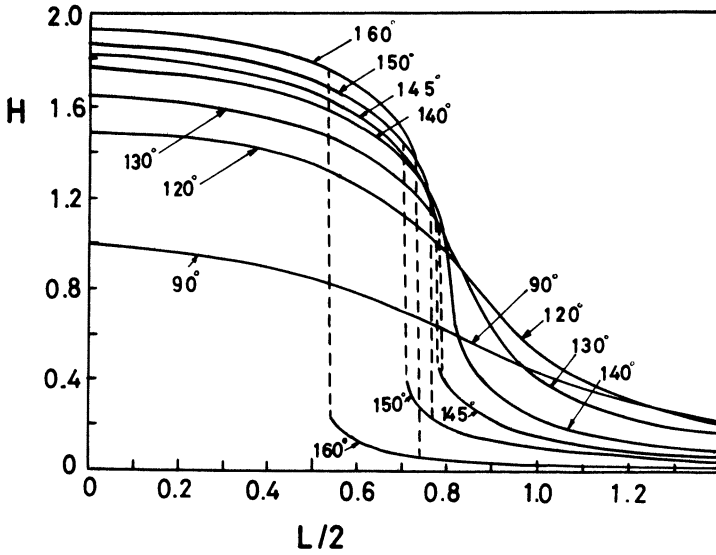FIGURE 15. *Cylindrical coordinate system for the example of R. Courant*

FIGURE 16. *The cross section at* $u = u_j$

The unknown variable z_i in this case is $R_{i,j}$, as shown in Fig. 16, and it is connected with $x_{i,j}$ and $y_{i,j}$ by

(4.1) $$x_{i,j} = R_{i,j} \cos \varphi_i, \qquad y_{i,j} = R_{i,j} \sin \varphi_i.$$

Hence,

FIGURE 17. *Relation between L and H*

$$(4.2) \quad \frac{\partial \bar{J}u}{\partial R_{i,j}} = \frac{\partial \bar{J}u}{\partial x_{i,j}} \frac{dx_{i,j}}{dR_{i,j}} + \frac{\partial \bar{J}u}{\partial y_{i,j}} \frac{dy_{i,j}}{dR_{i,j}}$$

$$= \frac{\partial \bar{J}u}{\partial x_{i,j}} \cos \varphi_i + \frac{\partial \bar{J}u}{\partial y_{i,j}} \sin \varphi_i = 0.$$

For the comparison of a free boundary program and cylindrical coordinate system program ($u_i = Lj/12$, $\varphi_i = (\pi/2)i/15$), numerical results of height H and $\frac{1}{4}$ of the total area are given in Table 3, where $r = 1.0$, $\theta = 5\pi/6$ and L varies.

TABLE 3. *Comparison of two methods*

C: cylindrical coordinate system
F: free boundary program

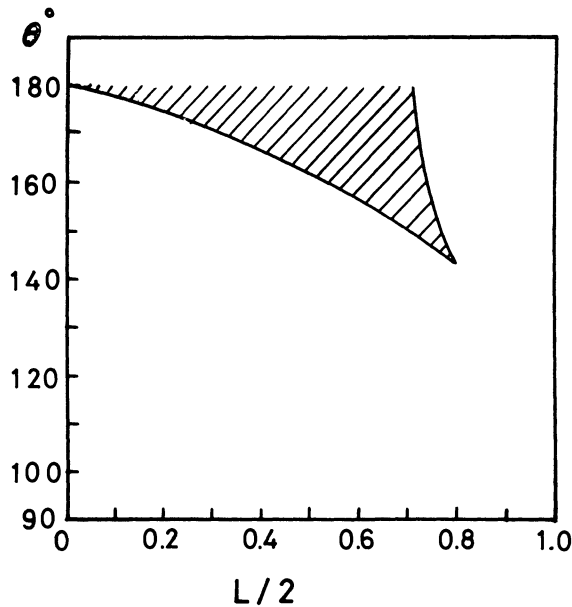| $L/2$		H	$\frac{1}{4}$ of the total area
0.7	C	1.447441	1.678319
	F	1.448845	1.678424
0.75	C	1.256070	1.766360
over	F	1.260619	1.766551
0.75	C	0.254281	1.754237
under	F	0.262425	1.756422
0.8	C	0.2141318	1.782874
	F	0.197830	1.785275

FIGURE 18. *The region where two different solutions exist*

As shown in Table 3, the two values of $\frac{1}{4}$ of the total area by the two methods are in mutual agreement within 0.2% relative error and the values of H within 3.5% for $L/2 \leq 0.75$ and 8.3% for $L/2 = 0.8$. This fact would imply that the solution to Courant's problem presented here has sufficient accuracy.

5. Result of a More General From of R. Courant's Problem. Next, consider a more general form of Courant's problem. Here, θ is also taken to be a variable as well as L. $r = 1.0$ was chosen.

Taking θ as a parameter, the relations between length L and height H are given in Fig. 17.

The region where the boundary has two solutions is given in Fig. 18.

6. Summary. It is shown that finite element methods are applicable to the Plateau problem. The variational direction suited to the problem can be selected in the finite element method and even the free boundary problem, which has been difficult to solve numerically, can be solved by the finite element method.

Even though the error analysis of the method presented here is yet to be fully examined, the examples considered give an insight into the accuracy of the computer program presented here. It is considered that the method has sufficient accuracy from a practical point of view.

All the computations were carried out using the FACOM 230-60 computer system at the Data Processing Center, Kyoto University.

The authors would like to express their gratitude to the referee for his valuable comments.

Central Research Laboratories
Nippon Electric Company Ltd.
Kawasaki, Japan

Department of Information Science
Kyoto University
Kyoto, Japan

Department of Information Science
Kyoto University
Kyoto, Japan

1. R. COURANT, *Dirichlet's Principle, Conformal Mapping, and Minimal Surfaces,* Interscience, New York, 1950. MR **12,** 90.
2. G. E. FORSYTHE & W. R. WASOW, *Finite-Difference Methods for Partial Differential Equations,* Appl. Math. Series, Wiley, New York, 1960. MR **23** #B3156.
3. D. GREENSPAN, "On approximating extremals of functions. I: The method and examples for boundary value problems," *ICC Bull.,* v. 4, 1965, pp. 99–120. MR **32** #8526.
4. D. GREENSPAN, "On approximating extremals of functions, Part II: Theory and generalization related to boundary value problems for nonlinear differential equations," *Internat. J. Engineering Sci.,* v. 5, 1967, pp. 571–588. MR **36** #3508.
5. P. CONCUS, "Numerical solution of the minimal surface equation," *Math. Comp.,* v. 21, 1967, pp. 340–350. MR **37** #4968.
6. R. STEPLEMANN, "Finite dimensional analogues of variational problems in the plane," *SIAM J. Numer. Anal.,* v. 18, 1971, pp. 11–23.